Effects of a newly incorporated stress-weakening term in a revised RSF on earthquake nucleation

Nobuki Kame[1,*], Satoshi Fujita[1], Masao Nakatani[1], Tetsuya Kusakabe[1]

[1] Earthquake Research Institute, the University of Tokyo, Tokyo 113-0032, Japan
* Corresponding author: kame@eri.u-tokyo.ac.jp

Abstract Quasi-static nucleation on a frictional fault embedded in an elastic medium is known to be sensitive to the frictional properties. Earlier works have employed 'aging' and 'slip' versions of rate- and state-dependent friction (RSF) law, but some clear flaws have been known; the aging law wrongly predicted linearly increasing slip-weakening distance with the amount of strength reduction, whereas the slip law could not reproduce observed time-dependent healing at very low velocities. Recently Nagata et al. [1] proposed a revised version of RSF by incorporating a stress-weakening effect newly found in laboratory experiments and by correcting the frictional parameters '*a*' and '*b*' largely, where '*a*' and '*b*' are the coefficients of RSF. It seems to be free from the previously known flaws and we here reexamined nucleation by using the revised RSF. From numerical simulations, two major differences were found. 1) For weakly velocity-weakening range of $0.85<a/b<1$, nucleation has characteristics of both unidirectional slip-pulse regime found in the slip law case and crack-like expansion regime in the aging law case. 2) Fixed-length patch regime occurs over a wider condition of a/b up to 0.85 in contrast with the previously reported range of $a/b<0.5$ implying strongly velocity-weakening faults.

Keywords Nucleation, Earthquake, Fault, Rate and State Friction

1. Introduction

On the basis of laboratory rock friction experiments the rate- and state-dependent friction law (RSF) was introduced [2]. It has been widely used in modeling of earthquake occurrence and successfully explained the mechanics of seismic cycles [3], aftershock activities [4] and many others. In the present paper, we focus on the modeling of earthquake nucleation by careful attention to the RSF formulae.

Quasi-static nucleation on a frictional fault buried in an elastic continuum is known to be sensitive to the frictional properties. Earlier works studied spontaneous nucleation under slow tectonic loading using 'aging' and 'slip' versions of rate- and state-dependent friction (RSF) law [5-7]. For strongly velocity-weakening faults characterized by $a/b<0.5$ ('*a*' and '*b*' are the coefficients of RSF), nucleation occurs in a 'fixed-length patch' regime, where regions of quasi-static slip remains relatively small. For weakly velocity-weakening faults ($0.5<a/b<1$), nucleation must propagate spatially (Fig. 1). Propagation occurs in a form of an expanding crack in the aging law case and in a form of a migrating slip pulse in the slip law case.

Both versions of RSF were proposed as descriptions of laboratory friction experiments, but some clear flaws are known; aging law's slip-weakening distance increases linearly with the amount of strength reduction, while slip law does not reproduce time-dependent healing at very low velocities. Recently Nagata et al. [1] proposed a revised version of RSF by incorporating a stress-dependent term with a coefficient '*c*' and by correcting the RSF parameters '*a*' and '*b*' largely. This new version of RSF seems to be free from the previously known flaws and is here employed to reexamine nucleation.

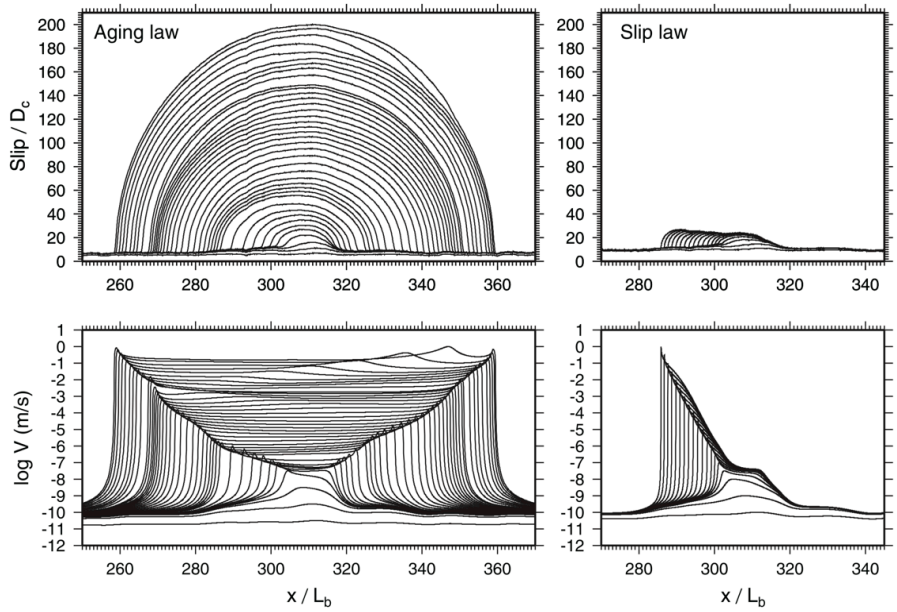

Figure 1. Snapshots of normalized slip (top panels) and slip rate (bottom) for two simulations identical in all respects except that the left panels use the aging law and the right panels the slip law. a/b=0.95, $D_c = 0.4\times10^{-3}$m , $V_0 = 10^{-9}$m/s , $\dot{\tau}_r = 10^{-2}$Pa/s, the normalizing length scale $L_b \equiv \mu_* D_c/(b\sigma) = 4.6$m. From figure 2 of Ampuero and Rubin [7] (in the present paper, the notation D_c is replaced by L).

1-1. Existing and revised RSFs

RSF consists of two equations bearing logically separate roles [8]. One is the constitutive law, which describes the relationship between applied shear stress τ and slip rate V as

$$V = V\exp\left(\frac{\tau-\Phi}{a\sigma}\right), \text{ or } \tau = \Phi + a\ln\left(\frac{V}{V_*}\right), \tag{1}$$

where Φ is the state variable specifying the internal physical state of the interface, which may reflect the real contact area [9], a is called direct effect coefficient and play an important role in the constitutive law for which the physical mechanism has been attributed to thermally activated creep [8,10], σ is a normal stress and V_* is a reference velocity. Another equation is the evolution law, which phenomenologically describes variations of the state Φ. Two empirical evolution equations for the evolution of Φ, first formalized by Ruina [11], are common use. These are

$$\frac{d\Phi}{dt} = \frac{b\sigma}{L}V_*\exp\left(-\frac{\Phi-\Phi_*}{b\sigma}\right) - \frac{b\sigma}{L}V \quad \text{(Aging law)}, \tag{2}$$

$$\frac{d\Phi}{dt} = -\frac{V}{L}\left(\Phi - \Phi_* - b\sigma\ln\left(\frac{V}{V_*}\right)\right) \quad \text{(Slip law)}\ , \tag{3}$$

where b is a RSF parameter relating change in state, L is a length scale related with slip, Φ_* is a reference state. The first and second terms of eq. (2) represent logarithmic time-dependent healing and linear slip weakening with a constant rate b/L per unit slip, while eq. (3) represents exponential slip weakening with a fixed distance L [8]. The aging law has trouble in reproducing a symmetric exponential change of friction over a fixed slip distance subsequent to stepwise velocity jumps to opposite signs observed in velocity-step tests (Fig. 2a) though it explains time-dependent healing in hold-slide tests very well as observed [8,11]. The slip law does explain the slip weakening (Fig. 2b), but has a well-known difficulty in reproducing time healing at low slip rate [12-13].

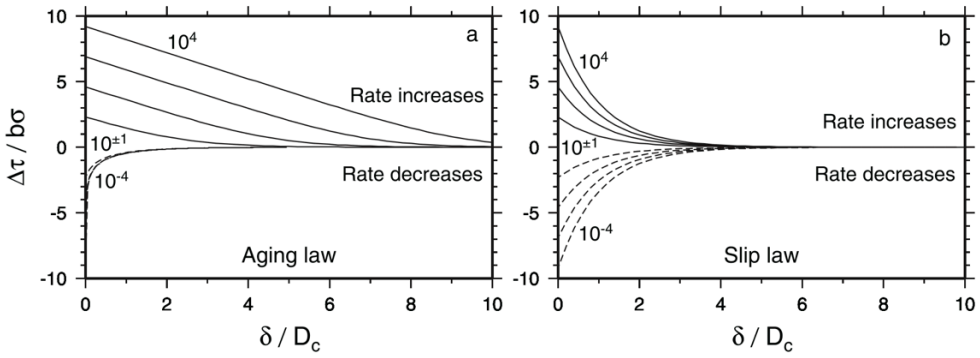

Figure 2. Plots of normalized stress as a function of normalized slip, for step velocity increases (solid lines) and decrease (dashed lines) of 1-4 orders of magnitude, for (a) the aging law and (b) the slip law. Stresses are relative to the future steady state value. For the aging law the curves for step decreases of 2-4 orders of magnitude appear indistinguishable, but they intersect the vertical axis at the same values of $\Delta\tau$ as the slip law. From figure 3 of Ampuero and Rubin [7] (in the present paper, the notation D_c is replaced by L).

Recently Nagata et al. [1] proposed a revised RSF, using new rigorous methods of laboratory data analysis. Firstly, the direct effect coefficient a was constrained to be 0.05, about five times larger than previously believed. The difference came from their new method to constrain a without using any evolution laws, contrasting to conventional methods where the state change from imperfection of real-world 'step' tests was inferred by assuming 'flawed' evolution law. This large a immediately led to similarly large $b \sim 0.05$ because $(b-a) \sim 0$ was reliably constrained from velocity dependence of steady-state friction without any evolution laws. Secondly, a strong linear negative dependence of $d\Phi/dt$ on $d\tau/dt$ was newly found from the misprediction analysis of Φ between the observed $\Phi(=\tau - a\ln(V/V_*))$ and the predicted Φ by using eq. (2). The shear-stress weakening effect was incorporated as

$$\frac{d\Phi}{dt} = \frac{b\sigma}{L} V_* \exp\left(-\frac{\Phi - \Phi_*}{b\sigma}\right) - \frac{b\sigma}{L} V - c\frac{d\tau}{dt} \quad , \tag{4}$$

where c is the stress weakening parameter. The term $-cd\tau/dt$ works to resolve the artifact of varying slip-weakening distance in the aging law as clearly seen in Fig. 3; when c=0, eq. (4) coincides with eq. (2) and the artifact remains unsolved, but with increasing c, the symmetric response in opposite sign of velocity-step tests was attained and the prediction curves became more symmetric like the slip law, keeping with the time-dependent healing term [14]. From the above misprediction analysis, the best-fit value of c was determined about 2.0. Nagata et al. [1] confirmed that the revised RSF could correctly reproduce both hold-slide and velocity-step tests with the same values of frictional parameters, which had never been attained in the existing RSFs. Very recently the revised RSF was employed to simulate earthquake cycle [15] and aftershock triggering [16].

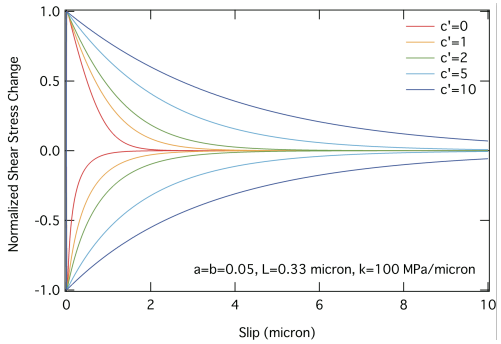

Figure 3. Normalized change of shear stress in velocity step-up and step-down tests predicted for different c. Slip rate is increased or decreased tenfold. From figure 5.21 of Nagata [14].

1-2. Nucleation regimes and lengths

We here briefly summarize nucleation regimes and their lengths in the previous studies [5-7] examined both numerically and analytically.

For strongly velocity-weakening faults characterized by a/b<0.5, nucleation occurs in a 'fixed-length patch' regime, where regions of quasi-static slip remains relatively small. In the patch regime, the state along patch kept well above steady state with insignificant healing. With a no-healing approximation, Rubin and Ampuero [6] analytically estimated the patch half-length as

$$L_v = 1.3774 L_b \qquad (L_b \equiv \frac{\mu_* L}{b\sigma}), \tag{5}$$

where $\mu_* = \mu/(1-\nu)$ is the stiffness of a medium for edge dislocation, μ is the rigidity, and ν is the Poisson's ratio. For the slip law, the patch length is slightly smaller than L_v [7].

For weakly velocity-weakening faults (0.5<a/b<1), nucleation must propagate spatially. Propagation occurs in a form of an expanding crack ('crack-like expansion' regime) in the aging-law case (Fig. 1a) and in a form of a migrating slip pulse ('unidirectional slip-pulse' regime) in the slip-law case (Fig. 1b). In the crack regime, the state along expanding portion instead kept steady state for increasing slip, that is, healing effect was not negligible. The nucleation half-length was estimated with a steady-state approximation as

$$L_\infty = \left(\frac{b}{b-a}\right)^2 \frac{L_b}{\pi} \qquad (b-a>0). \tag{6}$$

Ampuero and Rubin [7] attributed the crack-like expansion to the slip-weakening curves predicted with the aging law in response to velocity step ΔV (Fig. 2a), which would be experienced at the expanding nucleation front where the concentrated stress yields with a sudden jump in the slip rate. In their analysis, nucleation zone was proven to be approximated by a crack; stress uniformly drops by $\Delta\tau$ on the crack and locally concentrates at the tips by peak-to-residual stress drop $\Delta\tau_{p\text{-}r}$. Fracture mechanics tells us the energy release rate G in terms of the crack length l and fracture energy G_c at the crack tip, which were then connected to slip rate V on RSF faults as

$$G = \frac{\pi}{2}\frac{l}{\mu_*}(\Delta\tau)^2 \propto (\ln V)^2 \qquad (\Delta\tau \sim \sigma(b-a)\ln(V/V') - b\varepsilon) \tag{7}$$

$$G_c = \frac{\Delta\tau_{p-r}\delta_c}{2} = \frac{L}{2b\sigma}(\Delta\tau_{p-r})^2 \propto (\ln V)^2 \qquad (\Delta\tau_{p-r} \sim b\sigma\ln(V/V'') - \varepsilon) \tag{8}$$

where V' and V'' are nearly constant slip rates, δ_c is the effective slip-weakening distance following the linear slip-weakening rate *(b/L)*, and $\varepsilon \sim 0$. Setting $G = G_c$ and solving for the instantaneous nucleation length l lead to

$$l = \frac{L_b}{\pi}\left(\frac{\Delta\tau_{p-r}}{\Delta\tau}\right)^2 = l(V). \tag{9}$$

At every moment in accelerating V, the energy balance $G=G_c$ is satisfied; this is why the nucleation can be the crack-like expansion. By considering the ratio $\Delta\tau_{p\text{-}r}/\Delta\tau$ approaching *b/(b-a)* in the limit of large slip rate V, the nucleation size L_∞ in eq. (6) was derived. However, the prediction curves with increasing slip-weakening distances are an artifact due to the linear slip-weakening rate and contradict with laboratory experiments [8].

On the contrary, following the slip-weakening curves of the slip law (Fig. 2b), the fracture energy becomes $G_c \propto (\Delta\tau_{p-r})^1 \propto (\ln V)^1$ due to the constant slip-weakening distance, keeping $G \propto (\ln V)^2$ remain the same extent. The energy balance suggests that the accelerating V is incompatible with the crack-like expansion of the nucleation zone and numerical simulation demonstrated that the nucleation instead takes the form of unidirectional slip pulse (Fig. 1b). It must be noted that the nucleation was, however, wrongly predicted at the very beginning where the slip rate was very low and healing should have dominated. A genuine regime following laboratory experiments should be investigated by using the revised RSF.

2. Simulation method and choice of parameters

Following Dieterich [5], quasi-static nucleation is modeled here by adopting the revised RSF. A fault is divided by n equally spaced segment with a length Δs and loaded by a constant stressing rate $\dot{\tau}_r$:

$$\tau_i = \tau_i^0 + \dot{\tau}_r t + \Delta\tau_i \quad (i = 1,2,\cdots,n), \tag{5}$$

where τ_i is the shear stress, τ_i^0 is the initial stress, $\Delta\tau_i (= \Sigma S_{ij}\delta_j)$ is the change of stress resulting from the slip δ_j over the fault, and S_{ij} is stress kernel obtained from elastic dislocation solution [5]. By equating eq. (5) with eq. (1) and by substituting the revised law of eq. (4) to eliminate Φ, we obtain a couple of nondimensional differential equations:

$$d\tau_i'/dt' = \dot{\tau}_r' + S_{ij}' V_j' \tag{1.1}$$

$$d\left(\ln V_i'\right)/dt' = \left(a/b\right)^{-1}\left\{(1+c)d\tau_i'/dt' - \exp[-(\tau_i' - (a/b)\ln V_i')] + V_i'\right\} \tag{1.2}$$

where $\tau_i' = (\tau_i - \tau_*)/(b\sigma)$, $V_i' = V_i/V_*$, $t' = t/(L/V_*)$, $\dot{\tau}_r' = \dot{\tau}_r/(b\sigma/(L/V_*))$, $S_{ij}' = S_{ij}/(b\sigma)$ and frictional parameters (a,b,c,L) are assumed the same at all points on the fault. A factor ($1+c$) is newly appeared by the shear-stress dependent term. Nagata et al. [1] obtained a best fit parameter set (a,b,c,L)=(0.051, 0.0565, 2.0, 0.33micron) and this is the only set ever constrained by laboratory experiments. It leads to a/b=0.90 and ($1+c$)=3.0 in simulating nucleation.

In our controlled numerical experiments, c is chosen for a tuning parameter: no stress weakening c=0.0 is for the aging law, the optimum c=2.0 for the revised law, and an excessed c=4.0 for comparison. a/b is chosen as 0.95, 0.90, 0.85, 0.80, 0.75, implying that smaller a/b corresponds to stronger velocity weakening. Except for a/b and c, all simulations are identical in all respects. Fault discretization is done with n=2400 and $\Delta s = L_b/10$, small enough to resolve nucleation length. Initial velocity is assumed to be uniformly distributed $V_i'^0 = 1.0 (= V_*')$ and initial stress $\tau_i'^0$ is assumed to be randomly distributed between [-1,0] in order to start nucleation from below-steady state where the time-healing term dominates the slip-weakening term. $\dot{\tau}_r' = 0.1$ and $\mu_*' = 11.56\times10^3$ are chosen the same as in Ampuero and Rubin [7]. If $V_* = 10^{-9}$ m/s is taken, our simulation results are directly comparable with Fig. 1. Time integration is numerically done by using the Runge-Kutta method until $V_{\max}' = 10^9$.

3. Result

We conducted nucleation simulations with the total 15 sets of the revised RSF parameters (*a/b, c*) and found systematic changes in the results. Figure 4 shows the results with variation of *c*=0.0, 2.0, 4.0 under a fixed *a/b*=0.95, the snap shots of slip and slip rate evolution. When *c*=0.0 (the aging law) was adopted, a crack-like expansion occurred similar to Fig. 1a. Contrasting to this, when *c*=2.0, 4.0 were adopted, the crack-like propagation was completely disappeared. A narrow zone of peak slip velocity appears at the edge of the nucleation front propagating outwards like in the slip-law case, but the wide (and growing) region behind the front remains slipping at a velocity more than the 1/3 of the peak velocity, resulting in a slip distribution similar to that of an expanding crack as in the aging law case. Namely, the nucleation regime with the revised RSF was found to have both pulse feature in the spatial propagation and the crack feature in the slip rate distribution. The result may be understandable by comparing the revised law and the slip law. The revised law, as in the slip law favoring pulse, yields a slip-weakening distance nearly independent of the amount of strength reduction (Fig. 3), but it differs from the slip law in that it involves a time-dependent healing term, which should contribute significantly where the slip is proceeding near steady state. Crack-like extension would be no longer incompatible with the energy balance for instantaneous nucleation length *l* as pointed out in the section 1.2.

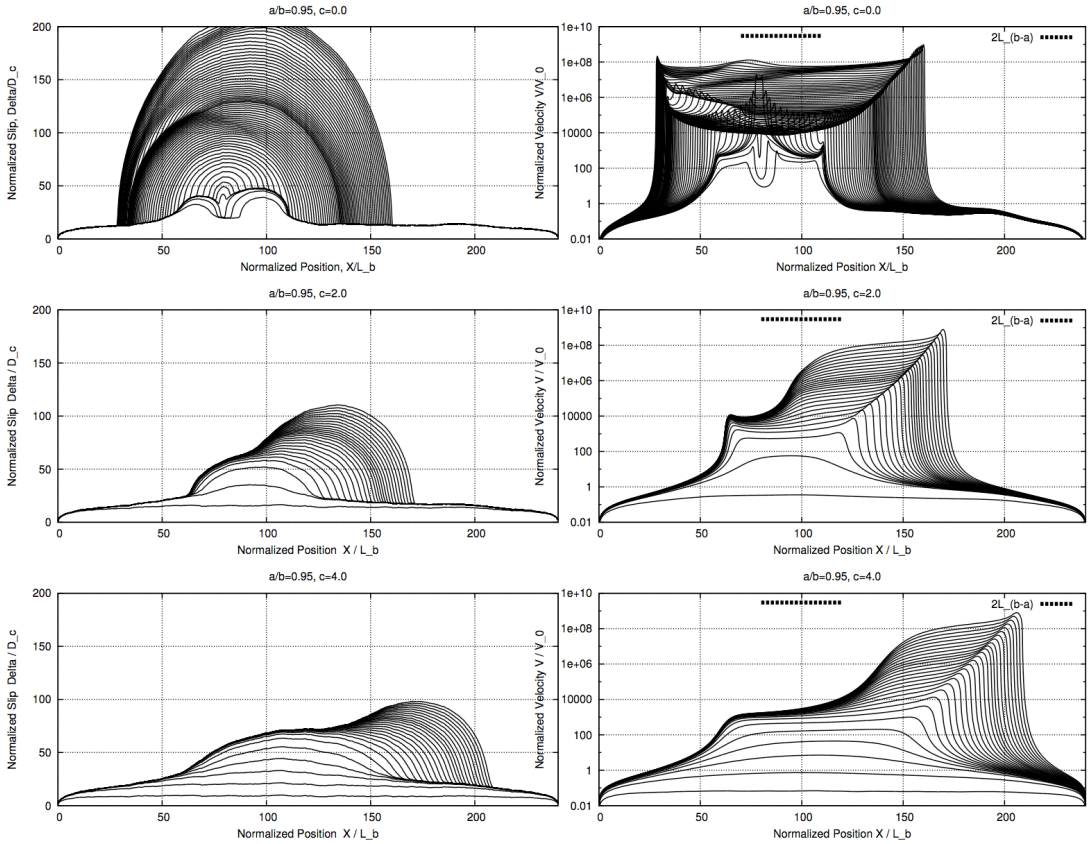

Figure 4. Snapshots of normalized slip (left panels) and slip rate (right panels) simulated by using the revised RSF for *a/b*=0.95 with three variations in the *c* parameter: (top) case with *c*=0.0, (middle) case with *c*=2.0, and (bottom) case with *c*=4.0.

Figure 5 shows the results with variation of *a/b*=0.90, 0.85, 0.80, 0.75 under fixed *c*=2.0 (the optimum) and *c*=4.0. Only snap shots of the slip rate are shown for brevity. For both *c*, transition from a pulse regime to a patch regime was observed as *a/b* was decreased. The transition was around *a/b*=0.80 for *c*=2.0 and *a/b*=0.85 for *c*=4.0, which are much larger than *a/b*=0.5 in the

previous studies as schematically summarized in Fig. 6. The condition for the patch regime widens as we increase a stress-weakening parameter *c*. As to the patch length with the revised RSF, it is obviously larger than the theoretical length $2L_v$ with the aging law in eq. (5) that is just a few digits ($\sim 2.7L_b$) in the normalized position in Fig. 5. The newly incorporated stress dependent term brought significant effects on the fixed-length path regime: the wider *a/b* range and the larger patch length. As to these results, a clear explanation has not been come up with.

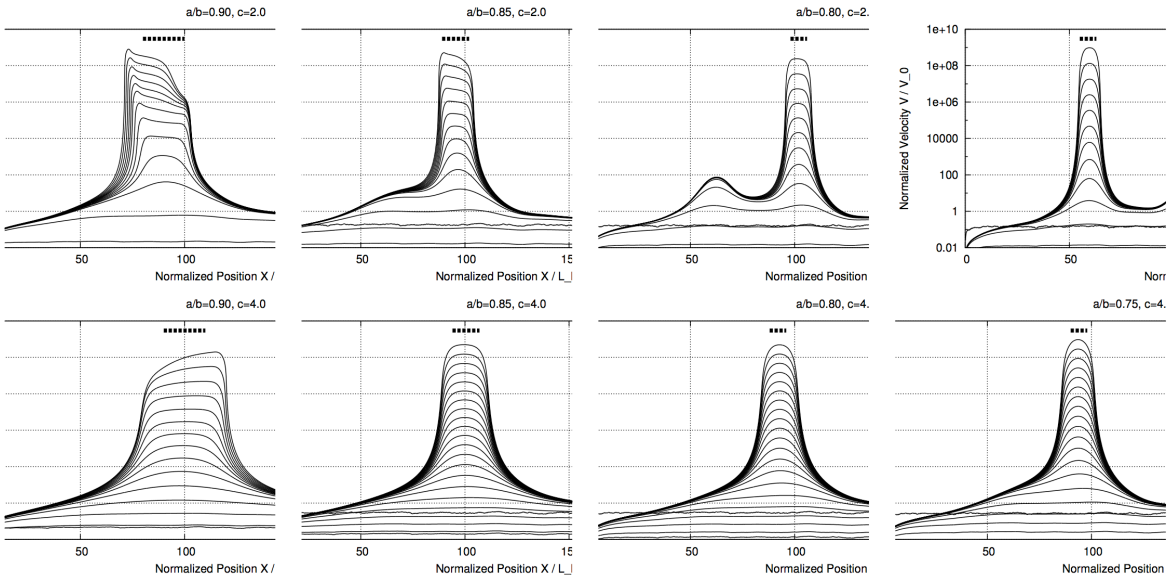

Figure 5. Snapshots of slip rate simulated with the revised RSF: (upper panels) cases with *c*=2.0, and (lower) cases with *c*=4.0 (from left to right: *a/b*=0.90, 0.85, 0.80, 0.75). All the vertical axes are in the same scale. A length scale $2L_{b\text{-}a}$ is plotted for reference by thick dashed line.

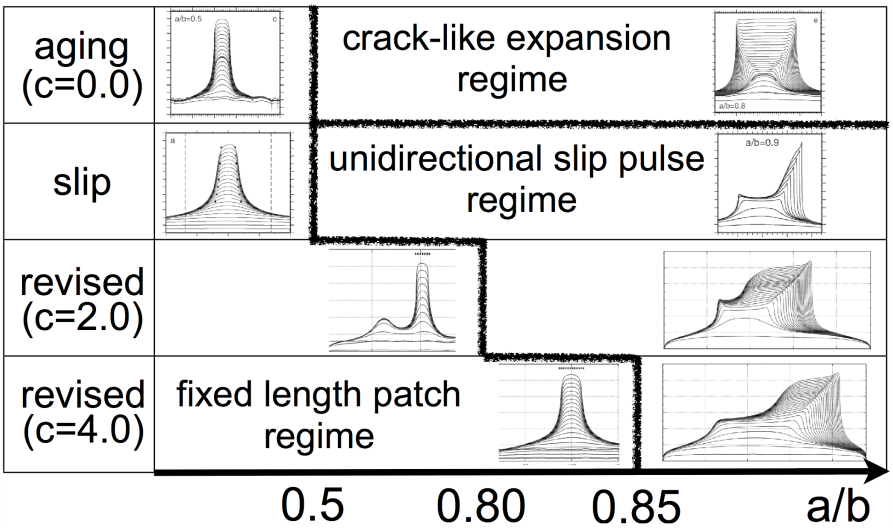

Figure 6. Nucleation regimes in 2-D simulation of quasi-static nucleation on RSF faults. The nucleation icons are from figure 1 of Rubin and Ampuero [6] in the aging law and figures 5 and 7 of Ampuero and Rubin [7] in the slip law.

4. Discussion

The simulated nucleation length was compared with the theoretically predicted value $2L_v$ and was found to be larger than $2L_v$. Seeking for a characteristic patch length with the revised RSF, we then compare it with another length scale

$$L_{b-a} \equiv \frac{\mu_* L}{(b-a)\sigma}, \tag{6}$$

where L_{b-a} is a characteristic nucleation length based on long-tem stick-slip instability [6]. $2L_{b-a}$ is plotted for reference by thick dashed line in Fig. 5. It seems to show a better agreement than $2L_v$ and may be a possible reference length at the moment. It is a tentative scale as a matter of course and future analytic work will be absolutely necessary to quantify the nucleation patch length explicitly including *c* parameter [17].

4. Conclusion

Nucleation on frictional faults was reexamined by using the revised RSF which seems to be free from previously known flaws. Our simulation results with systematic changes in the frictional parameter sets (*a/b,c*) comprehensively disclosed two major differences. 1) For weakly velocity-weakening range of $0.85<a/b<1$, nucleation had characteristics of both unidirectional slip-pulse regime found in the slip law case and crack-like expansion regime in the aging law case. 2) Fixed-length patch regime occurred over a wider condition of *a/b* up to 0.85 in contrast with the previously reported range of $a/b<0.5$ implying strongly velocity-weakening faults, and its patch length was larger than that predicted by the aging law.

Acknowledgements

N. Kato provided his numerical code. N.K. was supported by MEXT Grant-in-Aid for Scientific Research on Innovative Areas Number 21107007. This study was also supported by MEXT, under its Observation and Research Program for Prediction of Earthquakes and Volcanic Eruptions.

References

[1] K. Nagata, M. Nakatani, S. Yoshida, A revised rate- and state-dependent friction law obtained by constraining constitutive and evolution laws separately with laboratory data, J Geophys Res, 117 (2012) B02314 doi:10.1029/2011JB008818.
[2] J.H. Dieterich, Modeling of rock friction 1. experimental results and constitutive equations, J Geophys Res, 84 (1979) 2161-2168.
[3] S.T. Tse, J.R. Rice, Crustal earthquake instability in relation to the depth variation of frictional slip properties, J Geophys Res, 91 (1986) 9452-9472.
[4] J.H. Dieterich, A constitutive law for rate of earthquake production and its application to earthquake clustering, J Geophys Res, 99 (1994) 2601-2618.
[5] J.H. Dieterich, Earthquake nucleation on faults with rate- and state-dependent strength, Tectonophysics, 211 (1992) 115-134.
[6] A.M. Rubin, J.-P. Ampuero, Earthquake nucleation on (aging) rate and state faults, J Geophys Res, 110 (2005) B11312 doi:10.1029/2005JB003686.
[7] J.-P. Ampuero, A.M. Rubin, Earthquake nucleation on rate and state faults - Aging and slip laws, J Geophys Res, 113 (2008) B01302 doi:10.1029/2007JB005082.
[8] M. Nakatani, Conceptual and physical clarification of rate and state friction: Frictional sliding as a thermally activated rheology, J Geophys Res, 106 (2001) 13347-13380.

[9] J.H. Dieterich, B.D. Kilgore, Imaging surface contacts: power law contact distributions and contact stresses in quartz, calcite, glass and acrylic plastic, Tectonophysics, 256 (1996) 219-239.
[10] F. Heslot, T. Baumberger, B. Perrin, B. Caroli, C. Caroli, Creep, stick-slip, and dry-friction dynamics: Experiments and a heuristic model, Physical review E, 49 (1994) 4973-4988.
[11] A. Ruina, Slip instability and state variable friction laws, J Geophys Res, 88 (1986) 10359-10370.
[12] C. Marone, Fault zone strength and failure criteria, Geophys Res Lett, 22 (1995) 723-726.
[13] N. Kato, T.E. Tullis, A composite rate- and state-dependent law for rock friction, Geophys Res Lett, 28 (2001) 1103-1106.
[14] K. Nagata, Experimental study of friction behaviors using acoustic in-situ monitoring of frictional interface, Dr. Sc. Thesis, the University of Tokyo, 2008.
[15] N. Kame, S. Fujita, M. Nakatani, T. Kusakabe, Earthquake cycle simulation with a revised rate- and state-dependent friction law, Tectonophysics, (2012) doi: 10.1016/j.tecto.2012.11.029.
[16] N. Kame, S. Fujita, M. Nakatani, T. Kusakabe, Effects of a revised rate- and state-dependent friction law on aftershock triggering model, Tectonophysics, (2012) doi: 10.1016/j.tecto.2012.11.028.
[17] P. Bhattacharya, A.M. Rubin, Numerical and analytical study of rupture nucleation on 1D and 2D faults under a new state evolution law, AGU 2012 Fall Meeting abstract, S21B-2466, San Francisco.